International Journal of Adhesion & Adhesives 49 (2014) 33–37

Contents lists available at ScienceDirect

International Journal of Adhesion & Adhesives

journal homepage: www.elsevier.com/locate/ijadhadh

Montmorillonite reinforced phenol formaldehyde resin: Preparation, characterization, and application in wood bonding

Qun Fang [a,b,*], Hui-wang Cui [b,c,d,e,**], Guan-ben Du [b,c]

[a] School of Engineering, Zhejiang A & F University, Lin'an 311300, Zhejiang, China
[b] Southwest Forestry University, Kunming 650224, Yunnan, China
[c] College of Wood Science and Technology, Nanjing Forestry University, Nanjing 210037, Jiangsu, China
[d] Department of Material and Optoelectronic Science, National Sun Yat-Sen University, 804 Kaohsiung, Taiwan
[e] Institute of Scientific and Industrial Research, Osaka University, Ibaraki 565-0047, Osaka, Japan

ARTICLE INFO

Article history:
Accepted 30 September 2013
Available online 12 December 2013

Keywords:
Wood adhesives
Nano-composites
Adhesion

ABSTRACT

In this study, the montmorillonite (MMT) reinforced phenol formaldehyde (PF) resin intercalated nano-composite of PF–MMT was prepared from phenol, formaldehyde, and pristine MMT. We then introduced this PF–MMT into the production of plywood from Simao Pine veneers. Matrix assisted laser desorption ionization time of flight mass spectrometry (MALDI-TOF), wide-angle X-ray diffraction (XRD), differential scanning calorimetry (DSC), thermal mechanical analysis (TMA), and bonding strength revealed the related structure, curing, and mechanical properties. The thermoplastic PF with a linear structure entered the MMT layers and then formed the network structure after cured. The wet bonding strength and modulus of elasticity (MOE) of plywood were improved significantly. This preparation is simple and easy, and can be applied in the production of wood industry.

1. Introduction

Phenol formaldehyde (PF), because of its characteristics, such as economical on resources, easily produced, low cost, easy to apply, simple production technologies and equipment, and excellent mechanical properties, heat resistance, cold resistance, electrical insulation properties, dimensional stability, moldability, flame retardancy, and smoke resistance, etc., has been widely used in many industrial fields [1–3]. It can be divided as thermoplastic and thermosetting resins according to the different synthesis conditions. However, for the traditional, unmodified PF, a main weak link in the configuration is that the phenolic hydroxyl and methylene groups are easy to be oxidized which reduces the mechanical strength, heat resistance, and toughness, and also limits the related applications. Therefore, the modification or reinforcement of PF has been a hot research topic all the time, for example, the improvement on toughness [4–6], heat resistance [7–9], water resistance [10–12], and the reinforcement by nano-particles [13–15].

For further improvement of the properties and performance of PF, one of the most important technologies is the manufacture of (nano) composites through intercalating, blending, exfoliating, sol–gel, and molecular assembly with (organic) clay [16–19], but few specially focused on the application in wood bonding, especially in the production of plywood, particleboard, and fiberboard which are mainly used in wood industry. In our previous work, the exfoliated nano-composites from polyvinyl acetate and (organic) montmorillonite (MMT) were prepared and used in wood bonding successfully [20–25], and some exfoliated MMT nano-particles were obtained using a polyhedral oligomeric silsesquioxane surfactant and click chemistry [26]. On the basis of above research, the MMT reinforced PF intercalated nano-composite of PF–MMT was prepared from phenol, formaldehyde, and pristine MMT in this study (Scheme 1), and then it was introduced into the production of plywood from Simao Pine veneers. The structure, curing, and mechanical properties were investigated using matrix assisted laser desorption ionization time of flight mass spectrometry (MALDI-TOF), wide-angle X-ray diffraction (XRD), differential scanning calorimetry (DSC), thermal mechanical analysis (TMA), and bonding strength.

2. Experiment

2.1. Preparation of PF–MMT

About 1 mol of phenol, 0.35 mol of NaOH as a 30% aqueous solution, 1.2 mol of formaldehyde as a 37% formalin solution, and a certain weight of MMT were mixed together for 12 h under strong

* Corresponding author at: School of Engineering, Zhejiang A & F University, Lin'an 311300, Zhejiang, China. Tel.: +86 571 63732789; fax: +86 571 61062735.
** Corresponding author at: Institute of Scientific and Industrial Research, Osaka University, Ibaraki 565-0047, Osaka, Japan. Tel.: +81 6 68798521; fax: +81 6 68798522.
E-mail addresses: csqi2001@163.com (Q. Fang), cuihuiwang@hotmail.com (H.-w. Cui).

0143-7496/$ - see front matter © 2013 Elsevier Ltd. All rights reserved.
http://dx.doi.org/10.1016/j.ijadhadh.2013.12.011

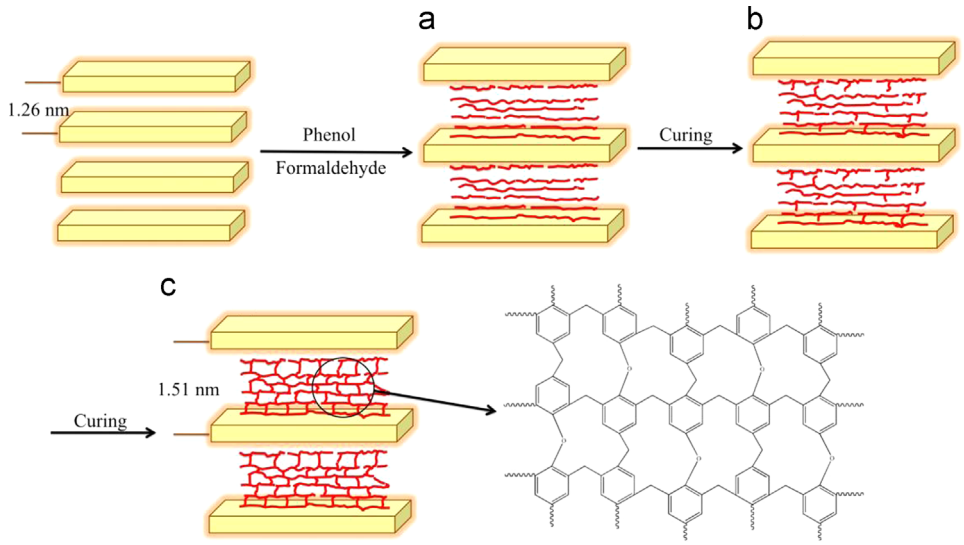

Scheme 1. Structural changes of PF–MMT during curing: (a) linear structure, (b) branched structure, and (c) network structure.

mechanical stirring at room temperature. Then the temperature rose slowly to reflux (94 °C) over a period of 30 min and under continuous stirring and kept at reflux for further 30 min. Hereafter, about 0.5 mol of formaldehyde as a 37% formalin solution was added. The reaction mix was now at pH 11 and the reaction continued at reflux until the resin achieved a specific viscosity between 500 mPa s and 800 mPa s. The PF–MMT resin was then cooled and stored. In the preparation, the MMT content was 1%, 2%, 3%, 4%, and 5% by the weight, and the corresponding PF–MMT was marked as PF–MMT-1%, PF–MMT-2%, PF–MMT-3%, PF–MMT-4%, and PF–MMT-5%, respectively. The PF resin was also prepared using the same method without MMT. The resin characteristics were then pH=11 and solids content=50% ± 1%.

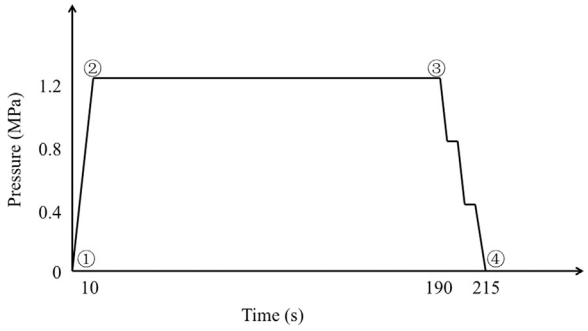

Fig. 1. Hot-pressing curve for plywood production.

2.2. Characterization

The MALDI-TOF spectra were recorded on a KRATOS Kompact MALDI 4 instrument. The irradiation source was a pulsed nitrogen laser with a wavelength of 337 nm. The length of one laser pulse was 3 ns. The measurements were carried out using the following conditions: polarity-positive, flight path-linear, mass-high (20 kV acceleration voltage), 100–150 pulses per spectrum. The delayed extraction technique was used applying delay times of 200–800 ns. The samples were dissolved in acetone (4 mg ml^{-1}). The sample solutions were mixed with an acetone/water solution (10 mg ml^{-1} acetone–water mix) of the matrix. 2,5-Dihydroxy benzoic acid was used as the matrix. For the enhancement of ion formation, NaCl was added to the matrix. The solutions of the sample and the matrix were mixed in equal amounts and 0.5–1 μl of the resulting solution were placed on the MALDI target. After evaporation of the solvent, the MALDI target was introduced into the spectrometer. Wide-angle X-ray diffraction data were collected using a Phillips X-ray diffraction. A triangular bent Si (111) single crystal was employed to obtain a monochromated beam having a wavelength (λ) of 1.54056 Å. The value of $d_{(001)}$ was calculated using Bragg's law, $\lambda = 2d \sin\theta$, where λ is the wavelength of the X-rays, d is the distance between two MMT layers, and θ is the diffraction angle. The curing of the samples was studied using a Perkin-Elmer differential scanning calorimeter operated under an atmosphere of pure N_2. The sample (ca. 7 mg) was placed in a sealed aluminum sample pan. The curing scans were conducted from 25 °C to 250 °C at a rate of 10 °C min^{-1}. The thermomechanical properties of the samples were tested using a Mettler 40 apparatus. Triplicate samples of beech wood alone, and of two beech wood plys each 0.6 mm thick bonded with each system, for a total samples dimensions of 21 mm × 6 mm × 1.2 mm were tested in nonisothermal mode between 40 °C and 220 °C at a rate of 10 °C min^{-1} in three-point bending on a span of 18 mm exercising a force cycle of 0.1/0.5 N on the specimens with each force cycle of 12 s (6 s/6 s). The classical mechanics relation between force and deflection $E=[L^3/(4bh^3)][\Delta F/\Delta f]$ allows the calculation of Young's modulus E for each case tested. The bonding strength was tested using a SHIMADUZ universal mechanical testing apparatus. The tested samples were plywood from Simao Pine (*Pinus kesiya Royle ex Gordon var. langbianensis* (*A. Chev*) *Gaussen*) veneers. The top, core, and bottom veneer all was 400 mm × 400 mm × 1.70 mm. The moisture content was about 10%. To produce the plywood, the PF and PF–MMT described above each was brushed on the veneer surface. The adhesive used was 120–150 g m^{-2}. Then these three brushed veneers were stacked together one on one. Their wood grain was perpendicular to each other. Lately, these stacked veneers were put into a Xinxieli BY302 × 2/15 hot-pressing machine. The hot pressure was 1.20 MPa, the hot-pressing temperature was 120 °C. As shown in Fig. 1, the pressure increased from 0 MPa to 1.20 MPa in 10 s from ① to ②; the pressure was kept stably at 1.20 MPa for 180 s from ② to ③, this stage was very important that the plywood was mainly produced in this stage; and in the next 25 s from ③ to ④, the pressure slowly decreased to 0 MPa step by step. Finally, the plywood was tested for dry bonding strength after cooled to room temperature. The plywood was made into the specimens of 80 mm × 25 mm × 8 mm. The bonding area was 60 mm × 25 mm. The specimens were then tested for dry bonding strength. For the

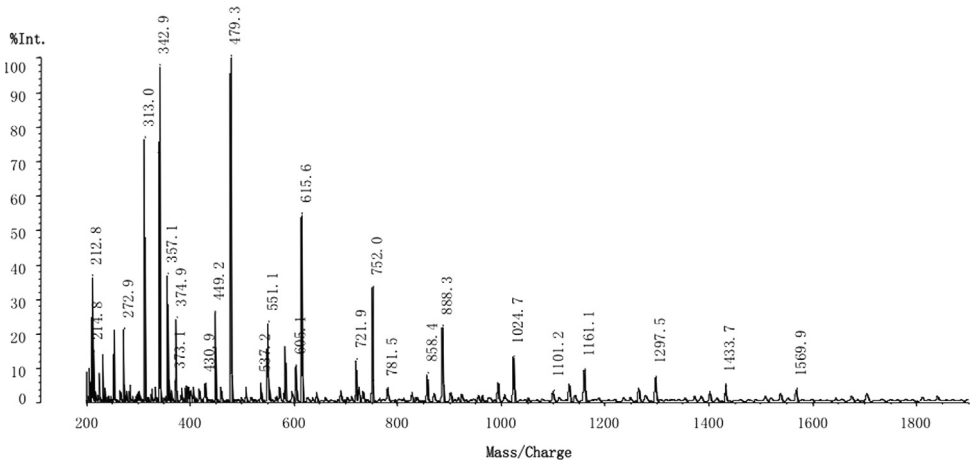

Fig. 2. MALDI-TOF spectrum of PF.

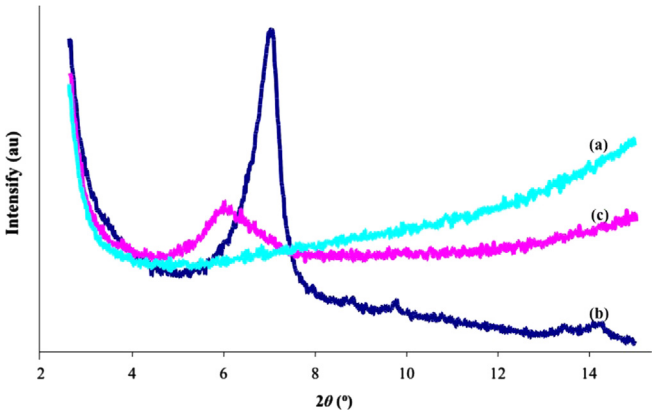

Fig. 3. XRD patterns of (a) PF, (b) MMT, and (c) PF–MMT.

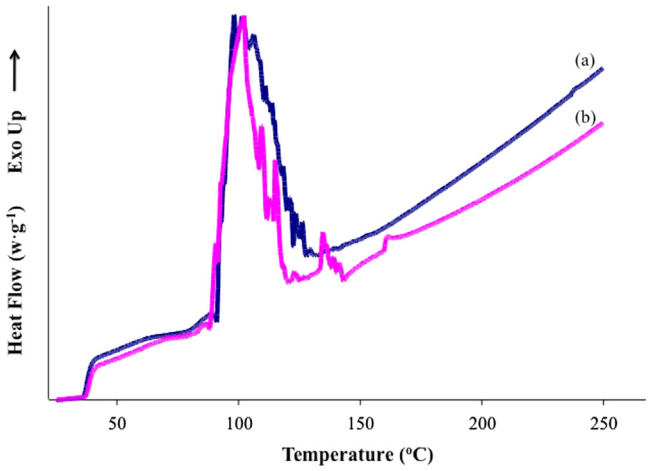

Fig. 4. DSC curves of (a) PF and (b) PF–MMT.

wet bonding strength, these specimens were immersed in 30 °C warm water for 3 h, and then in 20 °C cold water for 10 min. As these immersing finished, these specimens were tested at once for the wet bonding strength. The bonding strength was tested under a tensile rate of 10 mm min^{-1} at room temperature. The test should be finished in 10 min. 25 specimens were tested for each value.

3. Results and discussion

The MALDI-TOF result of PF in Fig. 2 shows the oligomers formed in a phenol–formaldehyde resin. It is noted that the predominant repeating unit was 136 Da representing the network structure for the thermosetting PF, and a few of repeating unit was 106 Da representing the linear structure for the thermoplastic PF. During the preparation of PF–MMT, only these a few of thermoplastic PF with a linear structure could enter the MMT layers easily, as shown in Scheme 1(a), while those thermosetting PF with a network structure not [27]. The thermoplastic PF with a linear structure entered, distracted, opened the MMT layers and formed the intercalated nano-composite of PF–MMT. As Fig. 3(a) shows, no diffraction peak appeared within the range 0.5–5° in the XRD patterns for PF. The XRD pattern of pristine MMT featured a peak at 7.03 °, corresponding to a basal space of 1.26 nm (Fig. 3(b)); that of the PF–MMT exhibited a diffraction angle at 5.87°, corresponding to a basal space of 1.51 nm—larger than that of pristine MMT. This observation implies that the thermoplastic PF with a linear structure had entered and opened the MMT layer to form the thermosetting PF with a network structure and a larger gallery distance after cured, as shown in Fig. 3(c), and Scheme 1(a)–(c).

The PF and PF–MMT had similar curing behaviors, but not exactly the same. As Fig. 4(a) shows, PF had a large, wide exothermic peak on the DSC curve representing the variation of PF from a linear structure to a branched structure and then to a network structure eventually. PF–MMT also had this variation. During the curing, the thermoplastic PF with a linear structure in MMT layers (Scheme 1(a)) firstly became the branched structure (Scheme 1(b)), and then the network structure eventually (Scheme 1(c)). However, it can be seen that PF–MMT had three exothermic peaks: one large, wide exothermic peak, and two small followed, as shown in Fig. 4(b). This is because the MMT sheets or layers in PF–MMT blocked the mass and heat transfer, delayed the curing [28–30], and some related different active energy reactions caused by this delaying effect appeared in the curing also [31].

As for the bonding strength, the plywood from Simao Pine veneers, PF, and PF–MMT was tested, and all the tested specimens were fractured at the bonding interface or in the wood veneers themselves. As Table 1 shows, the dry bonding strength was 1.97 MPa for PF, 1.86 MPa for PF–MMT-1%, 1.81 MPa for PF–MMT-3%, and 1.79 MPa for PF–MMT-5%. Apparently, MMT had no positive effect on the dry bonding strength. On the contrary, the wet bonding strength was improved significantly by MMT. They were 1.33 MPa, 1.61 MPa, 1.54 MPa, and 1.49 MPa respectively for PF, PF–MMT-1%, PF–MMT-3%, and PF–MMT-5%, as shown in Table 1. For PF–MMT, the bonding strength, including the dry and wet bonding strength, decreased with the MMT content increasing. Both reached the

Table 1
Bonding strength of PF and PF–MMT.

	Bonding strength (MPa)	
	Dry	Wet
PF	1.97	1.33
PF–MMT-1%	1.86	1.61
PF–MMT-3%	1.81	1.54
PF–MMT-5%	1.79	1.49

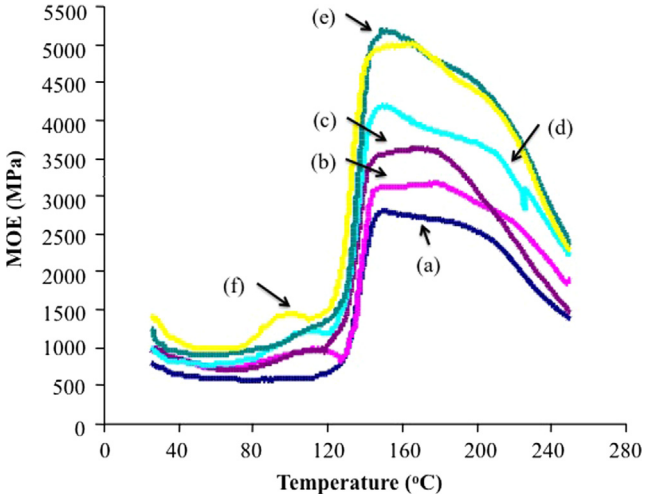

Fig. 5. MOE of (a) PF, (b) PF–MMT-1%, (c) PF–MMT-2%, (d) PF–MMT-3%, (e) PF–MMT-4%, and (f) PF–MMT-5%.

maximum value at PF–MMT-1% as 1.86 MPa for the dry bonding strength and 1.61 MPa for the wet bonding strength. The increment on the wet bonding strength was up to about 20% at PF–MMT-1% compared to that of PF.

Moreover, the MMT also reinforced the cohesion strength of PF, like the modulus of elasticity (MOE). As Fig. 5 shows, the MOE increased with the MMT content increasing, reached the maximum value at PF–MMT-4% (Fig. 5(e)), and then displayed little variation as the MMT increased continuously. The MOE of PF–MMT-5% (Fig. 5(f)) was almost the same as that of PF–MMT-4% (Fig. 5(e)). In PF–MMT, the MMT sheets or layers comprised some elementary particles (also called "structural units"), which were constituted by some thin solid layers. The MMT nanoparticles and the PF chains underwent an assembly process during the strong stirring used in the preparation of PF–MMT. The different charges of the components led to the formation of ionic bonds between them; this assembly process anchored these MMT sheets or layers with PF chains through physical crosslinking. The better the dispersion, the greater the number of physical crosslinking points and, therefore, the stronger the anchoring effect. In addition, because of the block effect on the mass and heat transfer from MMT, the PF molecules would have to move significantly to change the MOE by several orders of magnitude to show a significant variation. In other words, the structure of MMT, the assembly process, the anchoring effect, and the block effect all combined so that the PF–MMT systems possessed high wet bonding strength and MOE.

4. Conclusions

In this study, the MMT reinforced PF intercalated nanocomposite of PF–MMT was prepared from phenol, formaldehyde, and pristine MMT. We then introduced this PF–MMT into the production of plywood from Simao Pine veneers. The thermoplastic PF with a linear structure entered the MMT layers and then formed the network structure after cured. The wet bonding strength and MOE of plywood were improved significantly. The increment on the wet bonding strength was up to about 20% at PF–MMT-1%. This preparation is simple and easy, and can be applied in the production of wood industry.

Acknowledgment

The authors are grateful for the financial support of the National Nature Science Fundation of China (30930074).

References

[1] Higuchi M. Phenolic resin: alkali-catalyzed phenol–formaldehyde reactions. Mokuzai Gakkaishi 1999;45:425–33.
[2] Zmihorska-Gotfryd A. Coating compositions based on modified phenol–formaldehyde resin and urethane prepolymers. Prog Org Coat 2004;49:109–14.
[3] Fan Dong-bin, Qin Te-fu, Wang Chun-peng, Chu Fu-xiang. Evaluation of forestry residue-source oil-tea cake as an extender for phenol–formaldehyde plywood adhesive. For Prod J 2010;60:610–4.
[4] Cardona F, Ku H, Pattarachaiyakoop N, Rogers D, Trada M. Fracture toughness of phenol formaldehyde composites post-cured in microwaves. J Electromagn Wave Appl 2007;21:2137–46.
[5] Ku H, Rogers D, Davey R, Cardona F, Trada M. Fracture toughness of phenol formaldehyde composites: pilot study. J Mater Eng Perform 2008;17:85–90.
[6] Ku H, Cardona F, Pattarachaiyakoop N, Trada M. Fracture toughness of phenol formaldehyde composites reinforced with E-spheres. J Compos Mater 2009;43:741–754.
[7] Chernenko NM, Beilina NY, Sokolov AI. Technological aspects of heat resistance in carbon–ceramic composite refractories. Refact Ind Ceram 2009;50:149–52.
[8] Karaev SF, Bilalov YM, Naibova TM, Talybov GM, Nurieva UG. Protective polymer coatings based on phenol–formaldehyde oligomers modified by propargyl bromoethers. Prot Met Phys Chem Surf 2010;46:469–73.
[9] Lee Wen-Jau, Chang Kuo-Chun, Hsu Ling-Ying, Tseng I-Min. Properties of molding plates made with albizia wood particles impregnated with alcohol-soluble PF resins prepared from phenol-liquefied lignins. Holzforschung 2012;66:745–50.
[10] Ma Yuejia, Zhao Xu, Chen Xue, Wang Zichen. An approach to improve the application of acid-insoluble lignin from rice hull in phenol–formaldehyde resin. Colloid Surf A 2011;377:284–9.
[11] Wang Wenbo, Zhao Zongyan, Gao Zhenhua, Guo Mingruo. Whey protein-based water-resistant and environmentally safe adhesives for plywood. Bioresoures 2011;6:3339–51.
[12] Wang Wenbo, Zhao Zongyan, Guo Zhenhua, Guo Mingruo. Water-resistant whey protein based wood adhesive modified by post-treated phenol–formaldehyde oligomers (PFO). Bioresources 2012;7:1972–83.
[13] Lin RH, Fang L, Li XP, Xi YX, Zhang SF, Sun P. Study on phenolic resins modified by copper nanoparticles. Polym J 2006;38:178–83.
[14] Gao Jungang, Jiang Chaojie, Ma Weitao. Organic–inorganic hybrid boron-containing phenol–formaldehyde resin/SiO_2 nanocomposites. Polym Compos 2008;29:274–9.
[15] Sharma SK, Prakash J, Sudarshan K, Maheshwari P, Sathiyamoorthy D, Pujari PK. Effect of interfacial interaction on free volumes in phenol–formaldehyde resin–carbon nanotube composites: positron annihilation lifetime and age momentum correlation studies. Phys Chem Chem Phys 2012;14:10972–8.
[16] Gao Jungang, Jiang Chaojie, Su Xiaohui. Synthesis and thermal properties of boron–nitrogen containing phenol formaldehyde resin/MMT nanocomposites. Int J Polym Mater 2010;59:544–52.
[17] Lu Hongsheng, Li Guocheng, Dai Shanshan, Zhang Tailiang, Quan Hongpin, Huang Zhiyu. Synthesis and properties of aminoarylsulfonic acid–phenol–formaldehyde copolymer as drilling fluid loss reducer. J Macromol Sci Part A 2012;49:85–91.
[18] Bal A, Acar I, Guclu G, Iyim TB. Effects of organo clay on film properties of alkyd-phenol formaldehyde resins. Pigment Resin Technol 2012;41:100–3.
[19] Lopez Marta, Blanco Miren, Martin Maria, Mondragon Inaki. Influence of cure conditions on properties of resol/layered silicate nanocomposites. Polym Eng Sci 2012;52:1161–72.
[20] Cui HW, Du GB. Preparation and characterization of PVAc–MMT–DOAB. High Perform Polym 2011;23:40–8.
[21] Cui HW, Du GB. Rheology of PVAc–MMT–STAB. J Adhes Sci Technol 2011;25:1671–9.
[22] Cui HW, Du GB. Development of an exfoliated nanocomposite prepared by vinyl acetate and organic montmorillonite: structure, dynamic mechanical properties and thermal degradation. Compos Interfaces 2011;18:557–73.
[23] Cui HW, Du GB. Preparation and characterization of exfoliated nanocomposite prepared by vinyl acetate, montmorillonite and dioctadecyl dimethyl ammonium bromide. E-Polymers 2012;002:1–11.

[24] Cui HW, Du GB. Preparation and characterization of exfoliated nanocomposite of polyvinyl acetate and organic montmorillonite. Adv Polym Technol 2012;31:130–40.
[25] Cui HW, Du GB. Using Agrawal integral equation to study the glass transition and cold crystallization kinetics of exfoliated nano-composites synthesized by vinyl acetate and organic montmorillonite. J Compos Mater 2012;46:2951–8.
[26] Cui HW, Kuo SW. Using a polyhedral oligomeric silsesquioxane surfactant and click chemistry to exfoliate montmorillonite. RSC Adv 2012;2:12148–52.
[27] Jiang Wei, Chen Shinn-Horng, Chen Yun. Nanocomposites from phenolic resin and various organo-modified montmorillonites: preparation and thermal stability. J Appl Polym Sci 2006;102:5336–43.
[28] Gu AJ, Kuo SW, Chang FC. Syntheses and properties of PI/clay hybrids. J Appl Polym Sci. 2001;79:1902–10.
[29] Kuo SW, Huang WJ, Huang SB, Kao HC, Chang FC. Syntheses and characterizations of in situ blended metallocence polyethylene/clay nanocomposites. Polymer 2003;44:7709–19.
[30] Zhu Weijun, Lu Chu-Hua, Chang Feng-Chih, Kuo Shiao-Wei. Supramolecular ionic strength-modulating microstructures and properties of nacre-like biomimetic nanocomposites containing high loading clay. RSC Adv 2012;2:6295–305.
[31] He GB, Riedl B. Phenol–urea–formaldehyde cocondensed resol resins: their synthesis, curing kinetics, and network properties. J Polym Sci Part B 2003;41:1929–38.